Physical-World Attack towards WiFi-based Behavior Recognition

Jianwei Liu[1], Yinghui He[1], Chaowei Xiao[2], Jinsong Han[1,3], Le Cheng[1], and Kui Ren[1,3,4]

[1]Zhejiang University, China
[2]Nvidia Research and Arizona State University, USA
[3]Key Laboratory of Blockchain and Cyberspace Governance of Zhejiang Province, China
[4]Alibaba-Zhejiang University Joint Research Institute of Frontier Technologies, China

Abstract—Behavior recognition plays an essential role in numerous behavior-driven applications (*e.g.*, virtual reality and smart home) and even in the security-critical applications (*e.g.*, security surveillance and elder healthcare). Recently, WiFi-based behavior recognition (WBR) technique stands out among many behavior recognition techniques due to its advantages of being non-intrusive, device-free, and ubiquitous. However, existing WBR research mainly focuses on improving the recognition precision, while neglecting the security aspects. In this paper, we reveal that WBR systems are vulnerable to manipulating physical signals. For instance, our observation shows that WiFi signals can be changed by jamming signals. By exploiting the vulnerability, we propose two approaches to generate physically online adversarial samples to perform untargeted attack and targeted attack, respectively. The effectiveness of these attacks are extensively evaluated over four real-world WBR systems. The experiment results show that our attack approaches can achieve 80% and 60% success rates for untargeted attack and targeted attack in physical world, respectively. We also propose three methods to mitigate the hazard of such attacks.

Index Terms—Behavior recognition, WiFi, Genetic algorithm, Adversarial sample

I. INTRODUCTION

Behavior recognition is a key enabler for a wide range of essential human-centric applications (*e.g.*, virtual/augmented reality and smart home) and even the safety-critical applications (*e.g.*, healthcare and security surveillance). Traditional approaches utilize cameras [1], [2], sonar [3], [4], or wearable devices [5], [6] to capture behavior information, including gesture, activity, and the like. However, these approaches have their respective drawbacks, including the risk of visual privacy leakage, limited sensing range, and inconvenience inherent in using on-body sensor. Compared to these methods, WiFi-based solutions stand out by the advantages of being non-intrusive, contactless, device-free, and ubiquitous [7]–[20].

Existing WiFi-based behavior recognition systems extract behavior-relevant features from WiFi signals by measuring signals' channel state information (CSI). Previous studies of CSI-based behavior recognition system (termed as CBRS) focus on either improving the recognition accuracy or enabling the CBRS's environment-adaption ability [9], [14], while lacking the comprehensive exploration for its security issues. In fact, the security problem of CBRS is of essence,

Jinsong Han is the corresponding author.

because the recognition results are frequently related to the vital interests (*e.g.*, economic interest and life safety) of CBRS users. For instance, an adversary could manipulate certain wireless signals to mislead the decision of a fall detection system, threatening users' life safety. Even worse, in a smart home application, if an activity associated with turning the light on is falsely recognized as the activity of turning the gas on or opening the door, the user's life or property safety would be directly threatened.

Current CBRSes dominantly leverage machine learning-based methods for behavior recognition, but the emergence of adversarial samples severely threat the security of machine learning classifiers [21], [22], thus a natural concern arised: *Are these CBRSes vulnerable to practically physical adversarial samples? If so, to what extent?* In this paper, we study the security issue of CBRSes under adversarial environments by designing physical online attacks. To this end, we first explore the feasibility of manipulating the input CSI samples of CBRSes in the real world. We find that jamming signal could induce CSI absence in normal CSI samples due to the regulation of the CSMA/CA protocol [23]. The CSMA/CA protocol is adopted by network interface cards (NICs) in CBRSes and NICs control the transmission of signals. Therefore, it is possible to perform effective attacks by emitting jamming signals (standards-compliant WiFi signals) towards the transmitter of the CBRS, .

Although it is feasible to manipulate the input CSI, to achieve effective attacks is still difficult due to the following challenges: 1) *Stealthiness*: The attack should maintain the property of stealthiness so that the attack could not be easily detected by the CBRS user; 2) *Disdifferentiability*: Existing targeted attack methods mainly rely on adding perturbations to normal samples. The process of the perturbation optimization is differentiable. However, jamming signal changes the CSI in CBRS by causing CSI absence instead of adding perturbation, and this process is non-differentiable; 3) *Robustness*: To launch effective targeted attacks, the attacker should immediately emit jamming signals as long as the user starts to perform a behavior; otherwise, the attack will not jam the specified position in the normal CSI sample, resulting in the degradation of the attack effectiveness. Nevertheless, it is difficult to synchronize the jamming signal in the physical world. Besides,
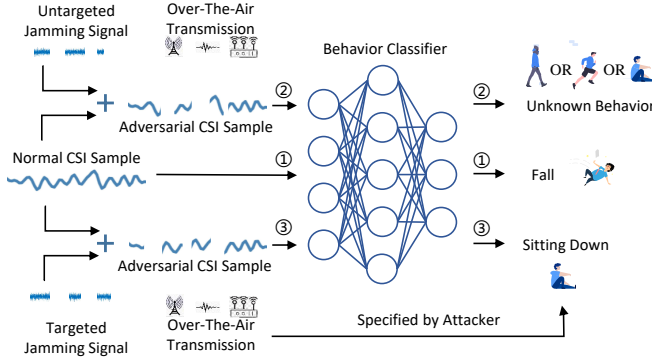
Fig. 1. Consequences of untargeted attack and targeted attack.

the CSI sample of a specific behavior is not unique. Therefore, the jamming signal designed for a known CSI sample may be ineffective to the one collected during online attack.

By overcoming the above challenges, we propose two approaches to launch physical-world untargeted and targeted attack against CBRSes, respectively. As shown in Fig. 1, the untargeted attack can lead the CBRS to recognize a behavior demonstrated by the user ('fall') as an unkown wrong one ('walk', 'run', or 'sit down'). The targeted attack can make the CBRS recognize the behavior ('fall') performed by the user as the one specified by the attacker ('sit down').

In detail, in order to overcome the first challenge, as our method exploits the CSI absence, we need to explore if the CSI absence also occurs in normal CSI samples. To this end, we first collect a large number of normal CSI samples and perform statistical analysis over them. We find that CSI absence exists in some normal CSI samples as well. In this case, as long as the degree of the CSI absence (*i.e.*, the number of absence times and the time length of each absence) caused by jamming signals is similar to that in normal CSI samples, the stealthiness of the attack can be guaranteed. Based on the result of this statistical analysis, we design an untargeted attack approach, in which we control the number of jamming times and the time length of each jamming to ensure sufficient stealthiness.

To address the second challenge, we first design an encoding scheme to encode jamming signals as bit sequences. With this scheme, we can leverage the genetic algorithm [24] consisting of three manipulation operations (duplication, crossover, and mutation) to optimize the jamming signal to generate targeted adversarial samples. As this optimization method does not require the differentiability, we can address the second challenge fundamentally.

To deal with the synchronization problem in the last challenge, we take the effect of the delay into account during optimization. We simulate the effect of delay by extending the fitness function in the genetic algorithm to a weight-based one. Moreover, to suppress the impact of the diversity of CSI samples, we introduce multiple CSI samples for each behavior when calculating the fitness score. Such countermeasure can help bit sequences improve their adaption abilities to the differences among different CSI samples.

In the evaluation part, we conduct comprehensive experiments on four CBRSes in real environments to study the effectiveness of our attack approaches. We invite 17 volunteers to collect both normal CSI samples and adversarial ones. The experiment results show that an attacker is able to achieve over 80% success rates in untargeted attacks. The success rate for targeted attack can reach 60%.

In summary, our contributions are as follows:

- We study the security issues of existing CBRSes in the physical world. To our best knowledge, we are the first to achieve both untargeted attack and targeted attack in CBRSes physically.
- We conduct comprehensive evaluation over four CBRSes. The results demonstrate that an attacker can achieve over 80% and 60% success rates on untargeted and targeted attacks, respectively.
- We show that our attack approaches can be easily generalized to other WiFi-based sensing applications, such as user authentication. Moreover, We propose three ways to mitigate the harmfulness of the attacks.

II. Background and Attack Feasibility

This section introduces the CBRS, the CSMA/CA protocol adopted by WiFi NICs, the formulation of the adversarial environments in CBRSes, and our threat model.

A. CSI-based Behavior Recognition

A CBRS usually contains two modules, *i.e.*, CSI acquisition and learning-based behavior classification [8]. Below, we introduce each module elaborately.

CSI acquisition: In a CBRS, users obtain behavior information by measuring CSI from WiFi signals. Since CSI describes how the signal experiences power attenuation and phase shift caused by human behavior, it can record abundant behavior information. Taking a CBRS with a transmitter and a receiver as an example, the transmitted signal s_{tx} is reflected/absorbed by human body and becomes s_{rx} at the receiver end. Then, the CSI H is estimated using known s_{tx} and s_{rx}. Since CBRS transmits signals with a unit of packet and a behavior usually takes a period of time, a behavior is recorded by a CSI sample containing the CSI of all packets transmitted during this period [25]. Therefore, a CSI sample has t rows and f columns of CSI value, where t is the number of packets and f is the number of used frequency. The CSI sample will be further processed in the next module.

Learning-based behavior classification: This module operates in two steps: *feature extraction* and *behavior classification*. In *feature extraction*, the CSI sample H extracted from the prior module first goes through some preprocesses (*e.g.*, low-pass filtering and interpolation [13], [15]). Then, an extraction method (*e.g.*, statistical scalar calculation [10]) is applied to the preprocessed H to get a feature vector x. Without loss of generality, we use $f_{ext}(\cdot)$ to represent the whole feature extraction process: $x = f_{ext}(H)$. In the second step, a machine learning classifier $F_w(\cdot)$ parameterized by w is built to map the feature vector x to the probabilities of a set of

labels. Each label corresponds to a category of behavior. The label that has the largest probability is the prediction result of $F_w(\cdot)$: $y = F_w(f_{ext}(H)) = F_w(x)$, where y is the predicted behavior label of x. To train the classifier, a batch of labeled CSI samples (*i.e.*, training set) is collected and the prediction error rate between the prediction label and ground-truth label is minimized. Once being well trained, the classifier can be used to predict the labels of unseen CSI samples, achieving the goal of behavior recognition.

B. CSMA/CA Protocol and CSI Absence

CSMA/CA protocol: NICs conform to the IEEE 802.11 a/b/g/n/ac/ax communication standard [26]. In these standards, CSMA/CA protocol is adopted to avoid collisions among signals at the same transmission channel but from different transmitters (each region in the world is allowed to use a specific number of channels [27] and each channel has f frequency). There are two main anti-collision mechanisms used by the CSMA/CA protocol: *carrier sensing* and *collision avoidance*. In a WiFi signal transmission task, the *carrier sensing* mechanism works at first. It lets the transmitter listen to the shared medium (*e.g.*, WiFi signals in the wireless network) to determine whether another transmitter is transmitting signals at the same channel or not. If the transmitter detects that the signal power of the same channel in the shared medium is larger than a threshold, the *collision avoidance* mechanism will stop the transmitter transmitting packets and wait for a period of time. After that, the transmitter will repeat the "*carrier sensing*"-"*collision avoidance*" loop until the shared medium is detected clear, *i.e.*, the sensed power of the signal at the same channel is smaller than the threshold. In the transmission process, the *carrier sensing* mechanism keeps working to guarantee that the transmitter stops transmitting once collision occurs in the shared medium.

CSI absence: As mentioned in Section II-A, each CSI sample is composed of CSI values of multiple packets over a period of time. In a CBRS, the time interval between any two consecutive packets approximates a constant value, *i.e.*, the transmitter sends packets at equal time intervals. In this way, each CSI sample can stably record the information of behavior. Suppose that the i_{th} transmission channel is used, the transmission rate is 100 packets per second, and each behavior continues for two seconds, then each CSI sample H should have dimensionality of (t, f). Ideally, t equals to 200 (100 packets/s $\times$ 2s). However, once we use another transmitter (attacker) to continuously emit signals (termed as jamming signals) at the i_{th} channel towards the CBRS's transmitter (victim), the aforementioned CSMA/CA protocol will stop the transmission of the victim transmitter. The victim transmitter will wait until the attacker transmitter stops the jamming. In this case, $t < 200$. That is, the number of rows in attacked CSI sample H' is less than 200, which means that some rows of the normal CSI sample are absent. This CSI absence caused by jamming signals makes the attack feasible as it manipulates H to H' ($H' \neq H$). In the remainder of this paper, the jamming

signal is denoted by s_j. The impact of the jamming signal to H is denoted as $J(\cdot)$ and we have $H' = J(H, s_j)$.

C. Behavior Recognition in Adversarial Environments

Given a classifier $F_w(\cdot)$, a feature vector x and its label y, an adversarial attacker launches an attack by generating an adversarial sample x', so that $F_w(x') \neq y$ (untargeted attack) or $F_w(x') = y'$ (targeted attack), in which y' is a targeted label. Prior works [21] have shown that the targeted attack can be achieved by generating an adversarial perturbation by optimizing the following objective function:

$$\min \quad ||x - x'||_p, \quad \text{s.t.} \quad F_w(x') = y' \text{ and } x' \in X, \quad (1)$$

where $F_w(x') = y'$ is the attack goal and $x' \in X$ means that the generated adversarial sample x' is in a valid set. Then, an optimization algorithm is leveraged to generate the perturbation. In a CBRS, the adversarial perturbation is indeed the jamming signal s_j. The objective function can be re-written as follows:

$$\min \quad ||f_{ext}(H) - f_{ext}(J(H, s_j))||, \quad (2a)$$
$$\text{s.t.} \quad F_w(f_{ext}(J(H, s_j))) = y' \text{ and } J(H, s_j) \in X.(2b)$$

In our attack scenario, as the jamming effect $J(H, s_j)$ is non-differentiable, we leverage the genetic algorithm to achieve the optimization objective.

D. Threat Model

Untargeted threat model: Untargeted attack attempts to fool the CBRS to output a false behavior label, which is not the one that the user demonstrated. In this threat model, the attacker does not need to have any prior knowledge about the CBRS. This model is a black-box one, which minimizes the constraints on the attacker. The attacker only needs to emit jamming signals towards the CBRS to influence its transmitter to launch attacks.

Targeted threat model: Targeted attack aims to mislead the CBRS to output a behavior label that is specified by the attacker. For the targeted attack, we have the following assumptions: 1) The attacker can detect when the CBRS user starts to perform an activity. This can be achieved by using WiFi-based behavior detection methods [28]; 2) We assume the targeted attack as a grey-box attack, *i.e.*, the attacker knows the detail of the feature extraction method $f_{ext}(\cdot)$ and the architecture of the targeted classifier. In fact, this is very nature since existing feature extraction methods and classifiers are public in the literature [13]–[15]. Note that the attacker does not need to know the detailed parameters of the classifier used by the victim CBRS.

III. UNTARGETED ATTACK

In this section, we introduce the approach for untargeted attack. An attacker can use NICs or software defined radios (SDRs) (*e.g.*, USRP [29]) to emit jamming signals. Besides, the attacker should know the WiFi transmission channel (target channel) used by the CBRS and the attack should not be easily detected, *i.e.*, the jamming signal should have stealthiness.
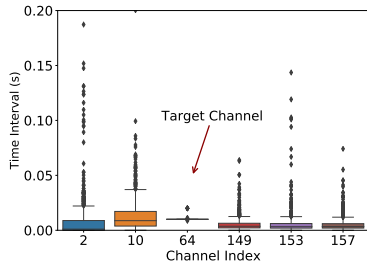
Fig. 2. Time interval distributions of CBRS and communication channels.

In the following sections, we first explain the reasons why the above requirements are necessary, and then introduce our designs to enable the attacker to meet these requirements.

A. Target Channel Determination

To jam the legitimate signal in a CBRS, the attacker needs to determine the channel used by the victim transmitter, *i.e.*, knowing the channel index (each permitted channel has a unique index). Intuitively, we can employ a NIC or SDR to collect signals around the CBRS to detect the channel index. However, there are many transmission channels used for daily communications in the ambient environments. As a result, the target channel might be overwhelmed by other irrelevant transmission channels, which confuses the attacker. Fortunately, to identify the target channel, the attacker can utilize the time interval between any two continuous packets to distinguish the target channel from other irrelevant ones. This is because such time intervals are stable in a CBRS but generally unstable in a communication system. To validate the feasibility of the above countermeasure, we first collect a batch of WiFi signals with different transmission channels around a CBRS, and then calculate the time intervals for each transmission channel. The box-plot of the time interval distributions are shown in Fig. 2. It can be observed that the time intervals of the target channel are significantly stable (with small box and a few black circles), while those of other transmission channels are unstable (with large box and lots of black circles). Therefore, the attacker can easily distinguish the target channel from other irrelevant ones according to the time interval.

B. Stealthiness of Attack

In order to launch attacks stealthily, a sophisticated attacker should make the jamming signal be effectively concealed, *i.e.*, the adversarial CSI samples should be difficult to distinguish from normal ones. Thus, we conduct an preliminary experiment to explore the feasibility for attackers to satisfy the stealthiness. In the experiment, we first collect over 2000 normal CSI samples in a normal laboratory environment from six reproduced CBRSes [7]–[11], [30]. Then we calculate the time intervals in each CSI samples. The experimental result shows that the CSI absence appears in over 50% normal CSI samples. The reasons causing this phenomenon are: 1) The reflection/absorption/occlusion of human body may hinder the signal propagation, resulting in the CSI absence in the received signals. This kind of CSI absence is also a kind
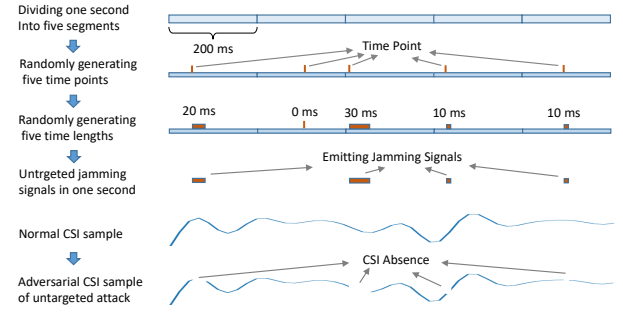

Fig. 3. Generation flow of untargeted jamming signals.

of feature of user behavior, because different behaviors cause different reflection/absorption/occlusion. 2) There are massive WiFi signals in the ambient environment. Some of them may be at the target channel, leading to the CSI absence in normal CSI samples. 3) With the hardware imperfection of the transmitter/receiver, some packets may not be successfully transmitted/received, which also induces CSI absence. Therefore, it is difficult for the CBRS to judge whether a CSI absence is induced by malicious jamming signals or other natural factors.

Afterwards, we count the number of CSI absence times in every one-second in each CSI sample. We find that the maximal frequency of CSI absence is smaller than 8 and most time lengths of CSI absences are less than 80 milliseconds. Therefore, similar to the X in Eq. 2, we define the *valid set*. In the valid set, each CSI sample contains no more than N_{abs} CSI absence times per second, and the time length of the longest CSI absence in this sample is less than T_{abs} milliseconds. In our experiments, we empirically set N_{abs} and T_{abs} as 8 and 80, respectively. Accordingly, to guarantee the stealthiness, the number of jamming attempts per second and each jamming duration should be smaller than N_{abs} and T_{abs} milliseconds, respectively. In this way, the generated adversarial CSI sample will fall into the valid set with large probability, and hence be indiscernible from normal CSI samples.

C. Attack Signal Generation

Our untargeted attack approach aims to achieve an attack that is imperceptible to users, while minimizing the requirements for attack. Thus, we opt to generate random jamming signals for untargeted attack. In this way, attackers do not need to have any prior knowledge about the target CBRS and the user cannot find the attack pattern. Based on the analysis in Section III-B, we summarize the untargeted jamming signal generation flow to the following steps: 1) Dividing one second into N_{abs} segments in the temporal domain. Each segment is $1/N_{abs}$ milliseconds. 2) Randomly generating N_{abs} jamming start time points (from t_s^1 to $t_s^{N_{abs}}$) for N_{abs} segments, the jamming signal will be emitted since the start time point. 3) Randomly generating N_{abs} jamming time lengths (from l_s^1 to $l_s^{N_{abs}}$) for N_{abs} segments, with each time length less than or equals to T_{abs} milliseconds. 4) In one second, the jamming signal is emitting at t_s^i for l_s^i milliseconds ($i \in [1, N_{abs}]$). A generation flow of the untargeted jamming signal generation is
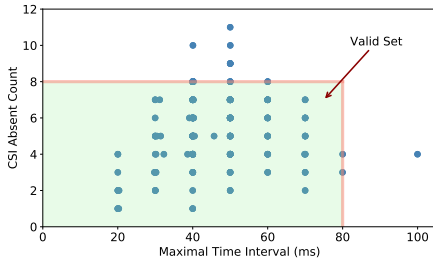
Fig. 4. CSI absence distributions of adversarial samples.

(a) Encoding scheme.   (b) Delay method.

Fig. 5. Jamming signal encoding scheme and delay method.

illustrated in Fig. 3. In this example, $N_{abs} = 5$ and $T_{abs} = 30$. To launch untargeted attacks at time t_{att}, an adversary only needs to repeat the last three steps since t_{att}.

The essential goal of the above flow is jamming the targeted channel stealthily. To validate its stealthiness, we invite volunteers to repeat three activities ('walk, sit, and fall') introduced in [10] and perform the untargeted attack. Meanwhile, we collect untargeted adversarial CSI samples (*i.e.*, the signal samples that under untargeted attacks). Then we show the time interval distributions of the adversarial CSI samples in Fig. 4. It can be observed that the majority of adversarial CSI samples lie in the valid set. Moreover, we found that the waveform of normal CSI sample is similar to that of adversarial one. Thus, the proposed untargeted attack conceals itself well.

IV. TARGETED ATTACK

In our targeted attack approach, an attacker can manually design a jamming signal $s_j^{a \to b}$, such that a CSI sample H^a of a specific behavior y_a can be classified as a target behavior y_b, *i.e.*, $y_b = F_w(f_{ext}(J(H^a, s_j^{a \to b})))$.

A. Methodology

To perform targeted attack, conventional approaches are to randomly generate a perturbation, and then leverage differentiable gradient descent to adjust its elements to optimize the perturbation. The perturbation can be added to normal samples to generate adversarial ones [21]. Nevertheless, these approaches cannot be used to generate $s_j^{a \to b}$ in our attack scenario, because what the adversary can do is to cause CSI absence (*i.e.*, element loss) of H^a, rather than increasing/decreasing its element values. More importantly, this process is non-differentiable.

To address this challenge, we opt to use the *genetic algorithm*. The core components of the genetic algorithm are how to calculate the *fitness score*, and how to encode and decode the *jamming signal*. If the genetic algorithm is used in our attack scenario, the attacker will generate better jamming signals (the signal with higher fitness score) and encoding them to feed into a fitness function (designed to calculate fitness score), until reach the optimum. The optimum is such a jamming signal that has the highest probability to mislead the behavior classifier to output a behavior label specified by the attacker.

Encoding scheme: To feed jamming signal into fitness function to calculate fitness score, we propose an encoding scheme for transforming the jamming signal $s_j^{a \to b}$. We observed that

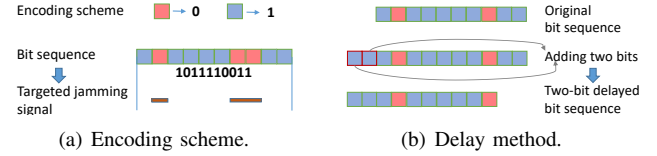each element in H^a is only in one of the two states, *i.e.*, either 'absent' or 'captured' during attack. In this case, the state of each element can be encoded as '0' (absent) or '1' (captured). Hence, the jamming signal can be represented by a bit sequence.

Suppose that the transmission rate of the victim transmitter is n_p packets per second and each behavior exists one second, each normal CSI sample would have n_p elements for each frequency. Moreover, since once a packet is not captured, the elements among all frequency channels correspond to this packet would be absent simultaneously. Without loss of generality, we assume that only one frequency is used by the victim transmitter to ease our following explanation. Under the above assumptions, the jamming signal can be encoded as a bit sequence that contains n_p bits. As shown in Fig. 5(a), a '0' in the bit sequence means the attacker transmitter emits jamming signals (making the element absent) and a '1' means the attacker transmitter stops jamming (making the element captured). The jamming function $J(\cdot)$ thus can be formulated as:

$$J(H^a, s_j^{a \to b}) = H^a \circ s_j^{a \to b}, \quad (3)$$

where $\circ$ is *Bitwise AND* operation [31].

Fitness score: In the genetic algorithm, each bit sequence is assigned with a fitness score to measure how close it is to the optimum. In our attack scenario, we regard the confidence coefficient calculated by the behavior classifier $F_w(\cdot)$ as the fitness score, because such confidence coefficient measures the probability that an input CSI sample should be classified as a behavior label. Therefore, a larger confidence coefficient means a larger probability, *i.e.*, a larger fitness score. The fitness score F^b of $s_j^{a \to b}$ can be calculated by:

$$F^b = Fit^b(F_w(f_{ext}(H^a \circ s_j^{a \to b}))) = Fit^b(H^a, s_j^{a \to b}), \quad (4)$$

where $Fit^b(F_w(\cdot))$ is the fitness function and it outputs the confidence coefficient of the behavior label y_b calculated by the behavior calssifier $F_w(\cdot)$.

B. Suppressing the Impact of Delay

So far, it seems that we can leverage the fitness function $Fit(\cdot)$ to optimize $s_j^{a \to b}$. However, certain delay exists in real-world attacks, *i.e.*, the normal CSI sample H^a and jamming signal $s_j^{a \to b}$ are not synchronized. This is because that even if the attacker instantly emits jamming signals once detects the beginning of a behavior, the time point that the jamming signals reach the victim transmitter would lag behind the beginning time point of the behavior. The lagging is induced by the propagation delay and hardware delay. The delay would make the received CSI sample not aligned with $H^a \circ s_j^{a \to b}$, and deteriorate the attack effectiveness.

To suppress the impact of delay, our solution is to enhance the fitness function. Specifically, the attacker can manually introduce a delay into the jamming signal during the optimization. The purpose is to improve the tolerance against the delay. As shown in Fig. 5(b), we deliberately generate a delay of n_d bits in a bit sequence through two steps: 1) Adding n_d '1' in the head of the bit sequence, so that the new bit sequence contains $n_d + n_p$ bits. 2) Removing n_d bits from the tail of the new bit sequence and a delayed bit sequence with n_p bits is finally obtained.

If we denote the function of delaying $s_j^{a \rightarrow b}$ for n_d bits as $D(s_j^{a \rightarrow b}, n_d)$, F_b is enhanced to a weighted fitness function as follow:

$$F^b = \sum_{i=0}^{n_d} \omega_i \cdot Fit^b(H^a, D(s_j^{a \rightarrow b}, i)), \qquad (5)$$

where $\omega_i \in [0, 1]$ denotes the weight for the i-bit delayed bit sequence and $\omega_i \geq \omega_{i+1}$. In the optimization process, F_b will continuously increase until the $s_j^{a \rightarrow b}$ approaches its optimum.

C. Jamming Signal Optimization

With the fitness function, the optimal $s_j^{a \rightarrow b}$, *i.e.*, the optimization objective (which is equivalent to the objective in Eq. 2) can be formulated as:

$$\max_{s_j^{a \rightarrow b}} \sum_{i=0}^{n_d} \omega_i \cdot Fit^b(H^a, D(s_j^{a \rightarrow b}, i)), \qquad (6a)$$

$$\text{s.t.} \quad J(H^a, s_j^{a \rightarrow b}) \in X. \qquad (6b)$$

Achieving this objective requires the following operations:

1) Initial generation: The attacker randomly generates N_b bit sequences that are in the valid set as the initial generation.
2) Fitness calculation: The attacker calculates the fitness score of every bit sequence in the generation.
3) Duplication: The attacker sorts the bit sequences according to their fitness scores. The top N_{dup} bit sequences are duplicated and the N_{dup} bit sequences with lowest fitness scores are removed.
4) Crossover: N_{cro} pairs of bit sequences are randomly selected from the generation to perform crossover. In each pair of bit sequences, we exchange their last n_{cro} bits.
5) Mutation: The attacker first randomly selects N_{mut} bit sequences, and then randomly selects n_{mut} bits from each of the N_{mut} bit sequences. The *Bitwise NEGATION* process [31] is then performed on these n_{mut} bits.

The first operation only needs to be performed once at the beginning of the optimization, yet the following four operations are alternately conducted in multiple iterations. A new generation will be produced in each iteration, which would be better than the previous generation. However, in practice, we find that a generation might degrade, *i.e.*, the sum of the fitness scores of current generation is smaller than that of the former generation after crossover and mutation. We term this phenomenon as degeneration. To deal with this degeneration problem, we introduce a mechanism that the crossover and mutation operations will be reconducted once degeneration
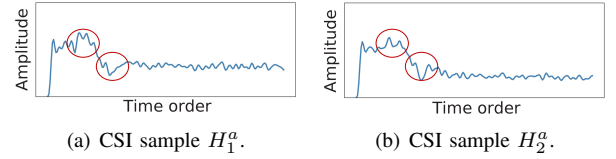

(a) CSI sample H_1^a. (b) CSI sample H_2^a.
Fig. 6. Two normal CSI samples of 'sit down' with small differences in red circles.

occurs. Moreover, in some generations the attacker might reconduct the crossover or mutation operation to guarantee that the bit sequence is in the valid set. The iteration will not stop unless the degeneration continuously occurs for N_{end} times. Empirically, N_{end} is set as 10. When the iteration terminates, we regard the bit sequence that has the largest fitness score as the optimum and decode it to obtain the final $s_j^{a \rightarrow b}$. In this way, the adversarial CSI sample generated by $J(H^a, s_j^{a \rightarrow b})$ is most likely to be classified as behavior y_b.

D. Attack Robustness Enhancement

In the real-world scenario, the H for a specific behavior is not unique. For example, two normal CSI samples of 'sit down' are presented in Fig. 6. We find that although the holistic profiles of the two curves are similar, their local profiles are different. In this case, the $s_j^{a \rightarrow b}$ generated for CSI sample H_1^a may be ineffective in attacking CSI sample H_2^a. To solve this practical problem, we further enhance the fitness function and objective function. Specifically, an attacker can first collect a batch of CSI samples containing that of behavior y_a to train the $F_w(\cdot)$. Then, the attacker can sum the fitness scores of all CSI samples of behavior y_a to improve the robustness of the generated jamming signal $s_j^{a \rightarrow b}$. If we denote the number of the CSI samples of y_a in the batch as n_{bat}, the enhanced fitness function can be formulated as:

$$F^b = \sum_{j=1}^{n_{bat}} \sum_{i=0}^{n_d} \omega_i \cdot Fit^b(H^{a_j}, D(s_j^{a \rightarrow b}, i)), \quad \text{s.t.} \quad \omega_i \in [0, 1]. \qquad (7)$$

The corresponding objective becomes:

$$\max_{s_j^{a \rightarrow b}} \sum_{j=1}^{n_{bat}} \sum_{i=0}^{n_d} \omega_i \cdot Fit^b(H^{a_j}, D(s_j^{a \rightarrow b}, i)), \qquad (8a)$$

$$\text{s.t.} \quad \omega_i \in [0, 1] \quad \text{and} \quad J(H^a, s_j^{a \rightarrow b}) \in X. \qquad (8b)$$

By using the batch and Eq. 7, the attacker can generate a more robust $s_j^{a \rightarrow b}$ to attack both H_1^a and H_2^a.

V. EVALUATION AND RESULT

Existing CBRSes can be divided into two categories according to whether the behavior classifier is based on deep neural network or not. We selected two representatives for each category and conducted experiments over them: WiFall [10], STFT [11], SignFi [9], and WiLSTM [7]. WiFall and STFT use random forest (RF) [32] and logistic regression (LR) [33] as behavior classifiers, respectively. The classifiers in SignFi and WiLSTM are most commonly used deep neural networks, *i.e.*, convolutional neural network (CNN) and long-short term memory (LSTM). These four systems can achieve significantly high behavior recognition accuracy.
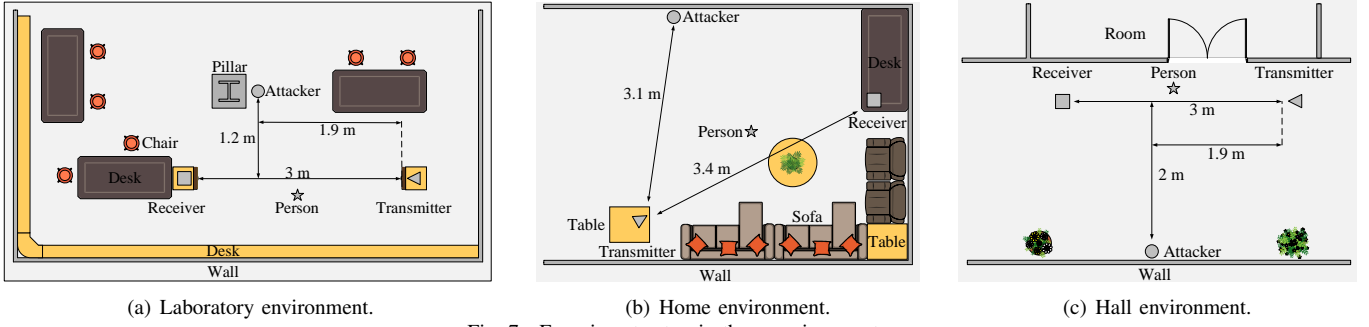
(a) Laboratory environment. (b) Home environment. (c) Hall environment.

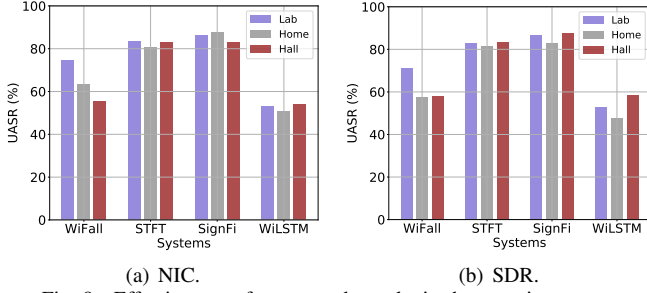Fig. 7. Experiment setup in three environments.

(a) NIC. (b) SDR.

Fig. 8. Effectiveness of untargeted attacks in three environments.
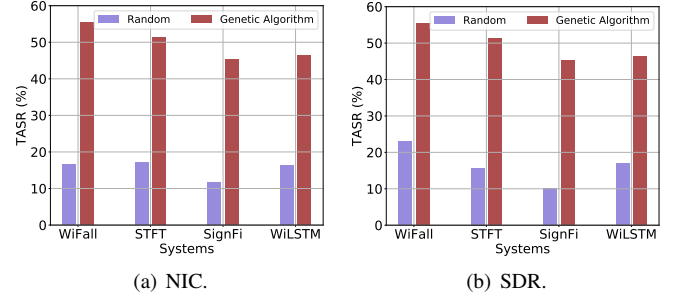

(a) NIC. (b) SDR.

Fig. 9. Effectiveness of our targeted attack approach ('Genetic Algorithm') and a baselines ('Random').

A. Experiment Setup and Metrics

Experiment setup: We reproduce four representative CBRSes and ensure that our implementation has comparable behavior recognition accuracy to the reference. We summarize the implementation details as follows: *WiFall.* In WiFall, six statistical features are calculated as the input of the behavior classifier. WiFall leverages RF to classify four activities including fall. The reference classification accuracy in [10] is 98.0%. Our reproduced WiFall achieves an accuracy of 98.5%. *STFT.* Frequency domain features are extracted as the input of classifiers in STFT. STFT can leverage LR to recognize six activities 'lie down, fall, walk, run, sit down, and stand up'. The highest reference classification accuracy in [11] is 90.5%. We reproduce STFT to have an accuracy of 99.7%. *SignFi.* Focusing on hand sign recognition, SignFi utilizes a CNN to classify the features containing both CSI amplitude and phase. We reproduced SignFi to recognize ten hand signs that represents ten numbers from zero to nine. The accuracy of our reproduced SignFi is 97.6%, while the accuracy reported in [9] is 97.2%. *WiLSTM.* The WiLSTM system utilizes an LSTM classifier and CSI amplitudes to recognize six activities similar to those in STFT. The reproduced WiLSTM has an equal accuracy with the reference, *i.e.*, 97.3% in [7].

As illustrated in Fig. 7, we implemented these systems under three different environments, including a laboratory, a home, and a hall. The victim transmitter was equipped with an Intel 5300 NIC and three antennas. The transmission rate of the CBRSes is 100 packets per second and each behavior lasts two seconds. For the attacker transmitters, we used both NIC (Atheros 9380) and SDR (USRP B210) to emit jamming signals. The jamming signals were modulated by *LabVIEW* [34]. We invited 17 volunteers (12 males and 5 females) aged

from 21 to 29 to collect CSI samples. In each environment, volunteers were asked to perform behaviors between the victim transmitter and receiver (with three antennas). The distance between the victim and attacker transmitters was about three meters. We totally collected 10932 normal CSI samples, 12639 CSI samples under untargeted attacks, and 27430 CSI samples under targeted attacks. We conducted the experiments by adhering to the approval of our university's Institutional Review Board (IRB).

Metrics: We defined two metrics to quantitatively measure the attack effectiveness: untargeted attack success rate (UASR) and targeted attack success rate (TASR). UASR is the probability that our jamming signals mislead the CBRS to output a false behavior label. It can be calculated by: $UASR = Acc_{nor} - \frac{N_{unt}^{cor}}{N_{unt}^{all}}$, where Acc_{nor}, N_{unt}^{cor}, and N_{unt}^{all} are the reproduced behavior recognition accuracy of our reproduced systems (*e.g.*, 98.5% in WiFall), the number of correctly classified untargeted adversarial CSI samples, and the number of all untargeted adversarial CSI samples, respectively. Similarly, TASR is the probability that a CSI sample of behavior y_a is classified as the behavior y_b when the victim transmitter is influenced by the targeted jamming signal $s_j^{a \to b}$. It can be calculated by: $TASR = \frac{N_{tar}^{cor}}{N_{tar}^{all}}$, where N_{tar}^{cor} and N_{tar}^{all} are the number of targeted adversarial CSI samples that are classified as the target behavior and the number of all targeted adversarial CSI samples of possible (y_a, y_b) pairs.

B. Overall Attack Effectiveness

To measure the effectiveness of our attack approaches, we first calculated the UASRs and TASRs for all volunteers, and then obtained the averages as the final results. The UASRs of NIC and SDR are shown in Fig. 8. It can be observed that,
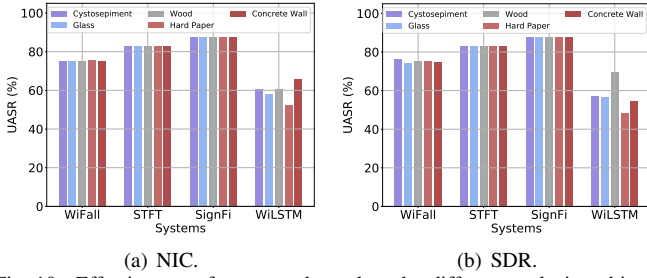
(a) NIC.

(b) SDR.

Fig. 10. Effectiveness of untargeted attack under different occlusion objects.

(a) NIC.

(b) SDR.

Fig. 12. Effectiveness of untargeted attack under different attack distances.

(a) NIC.

(b) SDR.

Fig. 11. Effectiveness of targeted attack under different occlusion objects.
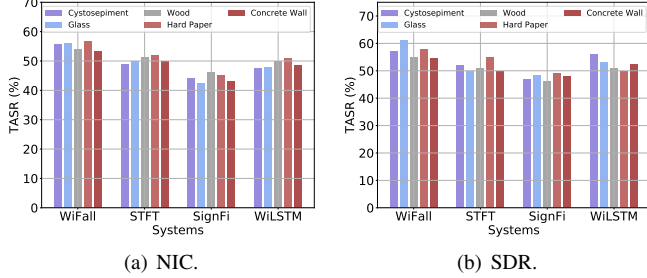

(a) NIC.

(b) SDR.

Fig. 13. Effectiveness of targeted attack under different attack distances.

with a NIC as the attacker transmitter, the highest UASRs for WiFall, STFT, SignFi, and WiLSTM can achieve 74.5%, 83.3%, 87.7%, and 54.0%, respectively. As for the SDR, the highest UASRs for the four systems are 71.0%, 83.4%, 87.6%, and 58.6%, respectively. Besides, there is no obvious UASR difference among the three environments. Especially, the high UASRs on the three environments indicate that our untargeted attack approach is significantly effective.

For the targeted attack, we averaged the TASRs over three environments and compared the targeted attack approach with a baseline, *i.e.*, the random jamming signal generation method in the untargeted attack approach. The results of NIC and SDR are shown in Fig. 9. 'Random' means the baseline and 'Genetic Algorithm' represents our targeted attack approach. It can be found that our targeted attack approach outperforms the baseline in all systems. The highest TASRs of NIC for these four systems are 56.0%, 52.5%, 46.3%, and 52.0% respectively. For the SDR, the highest TASRs for these systems are 60.0%, 55.0%, 48.5%, and 55.0% respectively.

C. Non-Line-Of-Sight Attack

In real-world attack scenarios, the main propagation path of signals between the victim transmitter and the attacker transmitter may be occluded by some objects. This attack scenario is called Non-Line-Of-Sight Attack (NLOS) attack. The power of jamming signals under this scenario would be reduced by the occlusion object. We also evaluate our approach in this extreme case. Specifically, we placed the attacker transmitter eight meters away from the victim transmitter and tested with five types of materials contained by the objects in our daily lives: cystosepiment, glass, wood, hard paper, and concrete wall. The thickness of them is 10.8, 0.5, 1.0, 2.5, and 28.0 centimeters respectively. The untargeted attack results of NIC and SDR are shown in Fig. 10. We can observe that the UASRs of different occlusion objects are similar, no matter we used NIC or SDR to emit jamming signals. The
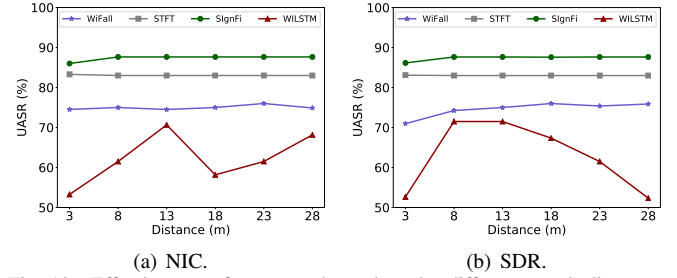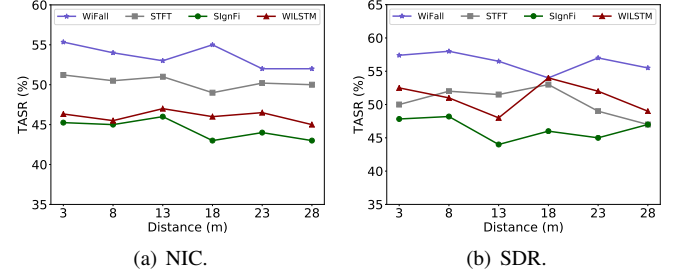
reason behind is that the jamming signal is utilized to stop the victim transmitter emitting signals, rather than change the values of normal CSI elements. As long as the power of the jamming signal is larger than the collision avoidance threshold of the victim transmitter, the attack can be successful. We also show the targeted attack results in Fig. 11, in which we can find that there is no obvious difference among different occlusion objects as well. Therefore, our attack approaches are still effective under occlusion conditions.

D. Impact of Distance

To explore the impact of the distance between the victim transmitter and the attacker transmitter, we changed the distance from three meters to 28 meters with a step of 5 meters. The UASRs of the NIC and SDR are shown in Fig. 12. Similar to the results of NLOS attack experiments, the distance (within 28 meters) has negligible effects on the attack effectiveness in WiFall, STFT, and SignFi. However, the UASRs of the WiLSTM system are unstable and jitter within the range from 52.3% to 71.5% randomly. This randomness is not induced by the distance variation, but the randomness in our untargeted jamming signal generation approach (introduced in Section III-C). The targeted attack results under different distances are shown in Fig. 13. Likewise, the distance does not affect the targeted attack effectiveness much. Therefore, an attacker is able to effectively launch long-distance untargeted and targeted attacks, while being hardly detected by CBRS users.

E. Transferability Study

We also evaluate the transferability of our adversarial samples. We train new classifiers with different architecture parameters among different tasks by following the standard setting [35], and then feed the previous adversarial samples into the new classifier. Specifically, we respectively used an RF classifier with 100 trees, a LR classifier with 'one vs. rest'

strategy, a four-layer CNN, and a Bi-LSTM to design jamming signals in WiFall, STFT, SignFi, and WiLSTM, while testing the attack effectiveness with an RF classifier with 50 trees, a LR with multinomial loss, a five-layer CNN, and an LSTM, respectively. The results show that the TASRs for the NIC are 50.6%, 42.0%, 30.8%, and 37.2% in WiFall, STFT, SignFi, and WiLSTM, respectively. Meanwhile, the TASRs of the SDR for these four systems are 53.0%, 45.6%, 32.5%, and 42.0% respectively. It can be found that the TASRs for WiFall, STFT, and WiLSTM only drop about 7%, which means that our targeted attack approach has decent transferability. Although the TASR of SignFi decreases a lot, it is still higher than 30.0%, which is also impactful in CBRS attacking.

VI. Mitigation

Geofencing WiFi Signals: Geofencing stops jamming signals from reaching the victim transmitter. A necessary of our attack approaches is that the power of jamming signals around the victim transmitter is larger than the collision avoidance threshold. Thus, geofencing, such as building walls with metal and painting walls with electromagnetic shielding paints, is an effective mitigation solution. However, it is undesirable to adopt geofencing as: 1) Geofencing also blocks legitimate WiFi signals, which affects the normal use of WiFi signals for communication. 2) Geofencing usually is costly. Strategic geofencing remains challenging.

Adversarial sample detection: This mitigation method protects the CBRS from attacks by determining if a collected CSI sample is an adversarial one. The potential adversarial CSI samples should be discarded to avoid the misclassification of the behavior classifier. Specifically, users can build a classifier to distinguish adversarial samples from benign ones. To evaluate the performance of this mitigation method, we trained a one-class support vector machine (SVM) [36] with the CSI values of normal CSI samples. The results show that the trained SVM can detect all adversarial CSI samples, which demonstrates that this mitigation method is effective in defending against our attack. Nevertheless, the SVM simultaneously rejected about 50% normal CSI samples, affecting the normal use of the behavior recognition system. Therefore, it is difficult to balance the usability and security while using this mitigation method.

Adversarial training: To mitigate the impacts of adversarial CSI samples, users can improve the robustness of the behavior classifier by adding adversarial CSI samples to the classifier's training set. In this way, the classification accuracy of adversarial CSI samples in WiFall, STFT, SignFi, and WiLSTM can achieve 65.0%, 68.8.0%, 75%, and 62.5%, respectively. However, adopting this mitigation method has to deal with a trade-off between the usability and security due to the following reasons: 1) Adding adversarial CSI samples into the training set brings massive extra overhead since users need to simulate the attack to collect adversarial CSI samples; 2) This mitigation method induces the degradation of normal CSI samples' classification accuracy, *e.g.*, a 13% decrease in STFT

system. Therefore, this mitigation should be further improved in defending against the proposed attacks.

VII. Related work

Behavior recognition systems have been widely deployed in many human-computer interaction applications. Traditional behavior recognition system usually is camera-, wearable-, phone-, or sonar-based [1]–[6], [37], [38]. For example, Guan *et al.* [6] proposed to use ensemble LSTM to improve the gesture recognition accuracy of individual LSTM on wearables. To enable non-intrusive and device-free human behavior recognition, WiFi-based solutions were proposed and developed rapidly. For instance, Guo *et al.* [12] have shown the feasibility of utilizing CSI amplitude and DT/RF/CNN/LSTM to accurately recognize activities. Nevertheless, previous works rarely paid attention to the security of the CBRS. In this paper, we explore the security of CBRS mainly from the perspective of an attacker.

WiFi-based attack techniques can be divided into active and passive ones according to whether the attack signal is emitted by the attacker or not. In the active attack, an attacker emits WiFi signals to sense physical-layer privacy of victims [39]–[41]. For example, Ali *et al.* [40] propose WiKey to sense a victim's keystroke. WiKey first emits WiFi signals towards the victim's keyboard, and then analyzes the signals reflected off the keyboard to infer the keystroke. In the passive attack, an attacker eavesdrops the WiFi signals emitted by victims and mine private information from these signals [28], [42], [43]. For instance, Cheng *et al.* [43] extract features from public WiFi signals to obtain WiFi users' privacy, such as identity, location, and financial privacy. To our knowledge, we are the first to achieve physical attacks towards CBRSes.

VIII. Conclusion

In this paper, we proposed two approaches to achieve untargeted attack and targeted attack against CBRSes, respectively. The experiment results on four real-world CBRSes demonstrated the high success rates of our attack approaches. Moreover, our attack approaches can be easily generalized to other WiFi-based sensing applications. At last, we discussed two methods to defend against the attacks.

REFERENCES

[1] G. Gkioxari, R. B. Girshick, P. Dollár, and K. He, "Detecting and recognizing human-object interactions," in *IEEE Conference on Computer Vision and Pattern Recognition, CVPR*, 2018, pp. 8359–8367.

[2] T. Li, Q. Liu, and X. Zhou, "Practical human sensing in the light," in *ACM International Conference on Mobile Systems, Applications, and Services, MobiSys*, 2016.

[3] K. Yatani and K. N. Truong, "Bodyscope: a wearable acoustic sensor for activity recognition," in *ACM Conference on Ubiquitous Computing Ubicomp*, A. K. Dey, H. Chu, and G. R. Hayes, Eds., 2012.

[4] R. Nandakumar, A. Takakuwa, T. Kohno, and S. Gollakota, "Covertband: Activity information leakage using music," *ACM on Interactive, Mobile, Wearable and Ubiquitous Technologies, IMWUT*, vol. 1, no. 3, pp. 87:1–87:24, 2017.

[5] A. Bulling, U. Blanke, and B. Schiele, "A tutorial on human activity recognition using body-worn inertial sensors," *ACM Computing Surveys*, vol. 46, no. 3, pp. 33:1–33:33, 2014.

[6] Y. Guan and T. Plötz, "Ensembles of deep LSTM learners for activity recognition using wearables," *ACM on Interactive, Mobile, Wearable and Ubiquitous Technologies, IMWUT*, vol. 1, no. 2, pp. 11:1–11:28, 2017.

[7] Z. Chen, L. Zhang, C. Jiang, Z. Cao, and W. Cui, "Wifi CSI based passive human activity recognition using attention based BLSTM," *IEEE Transactions on Mobile Computing, TMC*, vol. 18, no. 11, pp. 2714–2724, 2019.

[8] J. Ma, H. Wang, D. Zhang, Y. Wang, and Y. Wang, "A survey on wi-fi based contactless activity recognition," in *IEEE Conferences on Ubiquitous Intelligence & Computing, Advanced and Trusted Computing, Scalable Computing and Communications, Cloud and Big Data Computing, Internet of People, and Smart World Congress*, 2016.

[9] Y. Ma, G. Zhou, S. Wang, H. Zhao, and W. Jung, "Signfi: Sign language recognition using wifi," *ACM on Interactive, Mobile, Wearable and Ubiquitous Technologies, IMWUT*, 2018.

[10] Y. Wang, K. Wu, and L. M. Ni, "Wifall: Device-free fall detection by wireless networks," *IEEE Transactions on Mobile Computing, TMC*, vol. 16, no. 2, pp. 581–594, 2017.

[11] S. Yousefi, H. Narui, S. Dayal, S. Ermon, and S. Valaee, "A survey on behavior recognition using wifi channel state information," *IEEE Communications Magazine*, vol. 55, no. 10, pp. 98–104, 2017.

[12] L. Guo, S. Guo, L. Wang, C. Lin, J. Liu, B. Lu, J. Fang, Z. Liu, Z. Shan, and J. Yang, "Wiar: A public dataset for wifi-based activity recognition," *IEEE Access*, vol. 7, pp. 154 935–154 945, 2019.

[13] W. Jiang, C. Miao, F. Ma, S. Yao, Y. Wang, Y. Yuan, H. Xue, C. Song, X. Ma, D. Koutsonikolas, W. Xu, and L. Su, "Towards environment-independent device free human activity recognition," in *ACM International Conference on Mobile Computing and Networking, MobiCom*, 2018.

[14] Y. Zheng, Y. Zhang, K. Qian, G. Zhang, Y. Liu, C. Wu, and Z. Yang, "Zero-effort cross-domain gesture recognition with wi-fi," in *ACM International Conference on Mobile Systems, Applications, and Services, MobiSys*, 2019.

[15] W. Wang, A. X. Liu, M. Shahzad, K. Ling, and S. Lu, "Understanding and modeling of wifi signal based human activity recognition," in *ACM International Conference on Mobile Computing and Networking, MobiCom*, 2015.

[16] S. Ding, Z. Chen, T. Zheng, and J. Luo, "Rf-net: a unified meta-learning framework for rf-enabled one-shot human activity recognition," in *ACM Conference on Embedded Networked Sensor Systems, SenSys*, 2020.

[17] X. Zheng, J. Wang, L. Shangguan, Z. Zhou, and Y. Liu, "Smokey: Ubiquitous smoking detection with commercial wifi infrastructures," in *IEEE Conference on Computer Communications, INFOCOM*, 2016.

[18] C. Lin, T. Xu, J. Xiong, F. Ma, L. Wang, and G. Wu, "Wiwrite: An accurate device-free handwriting recognition system with COTS wifi," in *IEEE International Conference on Distributed Computing Systems, ICDCS*, 2020.

[19] X. Zheng, J. Wang, L. Shangguan, Z. Zhou, and Y. Liu, "Design and implementation of a csi-based ubiquitous smoking detection system," *IEEE/ACM Transactions on Networking, ToN*, vol. 25, no. 6, pp. 3781–3793, 2017.

[20] L. Zhang, Y. Zhang, and X. Zheng, "Wisign: Ubiquitous american sign language recognition using commercial wi-fi devices," *ACM Transactions on Intelligent Systems and Technology*, vol. 11, no. 3, pp. 31:1–31:24, 2020.

[21] Y. Cao, C. Xiao, B. Cyr, Y. Zhou, W. Park, S. Rampazzi, Q. A. Chen, K. Fu, and Z. M. Mao, "Adversarial sensor attack on lidar-based perception in autonomous driving," in *ACM SIGSAC Conference on Computer and Communications Security, CCS*, 2019.

[22] Q. Song, Z. Yan, and R. Tan, "Deep visual sensing against adversarial examples," *ACM Transactions on Sensor Networks, TOSN*, vol. 18, no. 5, pp. 1–32, 2022.

[23] IEEE, "IEEE standard for information technology—telecommunications and information exchange between systems local and metropolitan area networks," *IEEE Standard 802.11-2016 (Revision of IEEE Std 802.11-2012)*, pp. 1–3534, 2016.

[24] TutorialsPoint, "Genetic algorithm," https://www.tutorialspoint.com/genetic_algorithms/genetic_algorithms_introduction.htm, 2020.

[25] F. Wang, S. Zhou, S. Panev, J. Han, and D. Huang, "Person-in-wifi: Fine-grained person perception using wifi," in *IEEE/CVF International Conference on Computer Vision, ICCV*, 2019.

[26] D. Halperin, W. Hu, A. Sheth, and D. Wetherall, "802.11 with multiple antennas for dummies," *Computer Communication Review*, vol. 40, no. 1, pp. 19–25, 2010.

[27] N. Mostahinic and H. H. Refai, "Spectrum occupancy for 802.11a/n/ac homogeneous and heterogeneous networks," in *IEEE International Wireless Communications & Mobile Computing Conference, IWCMC*, 2019.

[28] Y. Zhu, Z. Xiao, Y. Chen, Z. Li, M. Liu, B. Y. Zhao, and H. Zheng, "Et tu alexa? when commodity wifi devices turn into adversarial motion sensors," in *Annual Network and Distributed System Security Symposium, NDSS*, 2020.

[29] C. Zhang, F. Li, J. Luo, and Y. He, "ilocscan: harnessing multipath for simultaneous indoor source localization and space scanning," in *ACM Conference on Embedded Network Sensor Systems, SenSys*, 2014.

[30] Q. Gao, J. Wang, X. Ma, X. Feng, and H. Wang, "Csi-based device-free wireless localization and activity recognition using radio image features," *IEEE Transactions on Vehicular Technology*, vol. 66, no. 11, pp. 10 346–10 356, 2017.

[31] Programiz, "Bitwiase operation," https://www.programiz.com/c-programming/bitwise-operators, 2020.

[32] L. Breiman, "Random forests," *Machine Learning*, vol. 45, no. 1, pp. 5–32, 2001.

[33] R. M. C. R. de Souza, D. C. F. Queiroz, and F. J. de A. Cysneiros, "Logistic regression-based pattern classifiers for symbolic interval data," *PATTERN ANALYSIS AND APPLICATIONS*, vol. 14, no. 3, pp. 273–282, 2011.

[34] LabVIEW, "The introduction of labview," https://www.ni.com/en-us/shop/labview.html, 2020.

[35] Y. Liu, X. Chen, C. Liu, and D. Song, "Delving into transferable adversarial examples and black-box attacks," *CoRR*, vol. abs/1611.02770, 2016.

[36] B. Schölkopf, R. C. Williamson, A. J. Smola, J. Shawe-Taylor, and J. C. Platt, "Support vector method for novelty detection," in *Advances in Neural Information Processing Systems, [NIPS Conference]*. The MIT Press, 1999, pp. 582–588.

[37] S. Shen, H. Wang, and R. R. Choudhury, "I am a smartwatch and I can track my user's arm," in *ACM International Conference on Mobile Systems, Applications, and Services, MobiSys*, 2016.

[38] J. Liu, X. Chen, S. Chen, X. Liu, Y. Wang, and L. Chen, "Tagsheet: Sleeping posture recognition with an unobtrusive passive tag matrix," in *IEEE Conference on Computer Communications, INFOCOM*, 2019.

[39] K. Chetty, G. E. Smith, and K. Woodbridge, "Through-the-wall sensing of personnel using passive bistatic wifi radar at standoff distances," *IEEE Transactions on Geoscience and Remote Sensing*, vol. 50, no. 4, pp. 1218–1226, 2012.

[40] K. Ali, A. X. Liu, W. Wang, and M. Shahzad, "Keystroke recognition using wifi signals," in *ACM International Conference on Mobile Computing and Networking, MobiCom*, 2015.

[41] B. Chen, V. Yenamandra, and K. Srinivasan, "Tracking keystrokes using wireless signals," in *ACM International Conference on Mobile Systems, Applications, and Services, MobiSys*, 2015.

[42] M. Li, Y. Meng, J. Liu, H. Zhu, X. Liang, Y. Liu, and N. Ruan, "When CSI meets public wifi: Inferring your mobile phone password via wifi signals," in *ACM SIGSAC Conference on Computer and Communications Security, CCS*, 2016.

[43] N. Cheng, X. O. Wang, W. Cheng, P. Mohapatra, and A. Seneviratne, "Characterizing privacy leakage of public wifi networks for users on travel," in *IEEE International Conference on Computer Communications, INFOCOM*, 2013.